The Monte Carlo simulation of the Borexino detector

S Marcocci[1,2,3]*

[1] Gran Sasso Science Institute, 67100 L'Aquila, Italy
[2] INFN, Laboratori Nazionali del Gran Sasso, 67010 Assergi (AQ), Italy
[3] Dipartimento di Fisica, Università degli Studi e INFN, 16146 Genova, Italy

E-mail: simone.marcocci@gssi.infn.it, simone.marcocci@ge.infn.it

M Agostini[1,2], **K Altenmüller**[4], **S Appel**[4], **V Atroshchenko**[5], **Z Bagdasarian**[6], **D Basilico**[7], **G Bellini**[7], **J Benziger**[8], **D Bick**[9], **G Bonfini**[2], **D Bravo**[10,7], **B Caccianiga**[7], **F Calaprice**[11], **A Caminata**[3], **S Caprioli**[7], **M Carlini**[2], **P Cavalcante**[2,10], **A Chepurnov**[12], **K Choi**[13], **L Collica**[7], **D D'Angelo**[7], **S Davini**[3], **A Derbin**[14], **X F Ding**[1,2], **A Di Ludovico**[11], **L Di Noto**[3], **I Drachnev**[1,2,14], **K Fomenko**[15], **A Formozov**[15,7,12], **D Franco**[16], **F Gabriele**[2], **C Galbiati**[11], **C Ghiano**[2], **M Giammarchi**[7], **A Goretti**[11], **M Gromov**[12], **D Guffanti**[1,2], **C Hagner**[9], **T Houdy**[16], **E Hungerford**[17], **Aldo Ianni**[2]†, **Andrea Ianni**[11], **A Jany**[18], **D Jeschke**[4], **V Kobychev**[19], **D Korablev**[15], **G Korga**[17], **D Kryn**[16], **M Laubenstein**[2], **E Litvinovich**[5,20], **F Lombardi**[2]‡, **P Lombardi**[7], **L Ludhova**[6,21], **G Lukyanchenko**[5], **L Lukyanchenko**[5], **I Machulin**[5,20], **G Manuzio**[3], **J Martyn**[22], **E Meroni**[7], **M Meyer**[23], **L Miramonti**[7], **M Misiaszek**[18], **V Muratova**[14], **B Neumair**[4], **L Oberauer**[4], **B Opitz**[9], **V Orekhov**[5], **F Ortica**[24], **M Pallavicini**[3], **L Papp**[4], **Ö Penek**[6,21], **N Pilipenko**[14], **A Pocar**[25], **A Porcelli**[22], **G Ranucci**[7], **A Razeto**[2], **A Re**[7], **M Redchuk**[6,21], **A Romani**[24], **R Roncin**[2,16], **N Rossi**[2], **S Schönert**[4], **D Semenov**[14], **M Skorokhvatov**[5,20], **O Smirnov**[15], **A Sotnikov**[15], **L F F Stokes**[2], **Y Suvorov**[26,5], **R Tartaglia**[2], **G Testera**[3], **J Thurn**[23], **M Toropova**[5], **E Unzhakov**[14], **A Vishneva**[15], **R B Vogelaar**[10], **F von Feilitzsch**[4], **H Wang**[26], **S Weinz**[22], **M Wojcik**[18], **M Wurm**[22], **Z Yokley**[10], **O Zaimidoroga**[15], **S Zavatarelli**[3], **K Zuber**[23], and **G Zuzel**[18] (Borexino Collaboration)

[4] Physik-Department and Excellence Cluster Universe, Technische Universität München, 85748 Garching, Germany
[5] National Research Centre Kurchatov Institute, 123182 Moscow, Russia
[6] IKP-2 Forschungzentrum Jülich, 52428 Jülich, Germany
[7] Dipartimento di Fisica, Università degli Studi e INFN, 20133 Milano, Italy
[8] Chemical Engineering Department, Princeton University, Princeton, NJ 08544, USA
[9] Institut für Experimentalphysik, Universität Hamburg, 22761 Hamburg, Germany
[10] Physics Department, Virginia Polytechnic Institute and State University, Blacksburg, VA 24061, USA
[11] Physics Department, Princeton University, Princeton, NJ 08544, USA
[12] Lomonosov Moscow State University Skobeltsyn Institute of Nuclear Physics, 119234 Moscow, Russia
[13] Department of Physics and Astronomy, University of Hawaii, Honolulu, HI 96822, USA

* Now at: Fermi National Accelerator Laboratory, Batavia, IL 60510, USA.

† Also at: Laboratorio Subterráneo de Canfranc, Paseo de los Ayerbe S/N, 22880 Canfranc Estacion Huesca, Spain.

‡ Present address: Physics Department, University of California, San Diego, CA 92093, USA.

[14] St. Petersburg Nuclear Physics Institute NRC Kurchatov Institute, 188350 Gatchina, Russia

[15] Joint Institute for Nuclear Research, 141980 Dubna, Russia

[16] AstroParticule et Cosmologie, Université Paris Diderot, CNRS/IN2P3, CEA/IRFU, Observatoire de Paris, Sorbonne Paris Cité, 75205 Paris Cedex 13, France

[17] Department of Physics, University of Houston, Houston, TX 77204, USA

[18] M. Smoluchowski Institute of Physics, Jagiellonian University, 30059 Krakow, Poland

[19] Kiev Institute for Nuclear Research, 03680 Kiev, Ukraine

[20] National Research Nuclear University MEPhI (Moscow Engineering Physics Institute), 115409 Moscow, Russia

[21] RWTH Aachen University, 52062 Aachen, Germany

[22] Institute of Physics and Excellence Cluster PRISMA, Johannes Gutenberg-Universität Mainz, 55099 Mainz, Germany

[23] Department of Physics, Technische Universität Dresden, 01062 Dresden, Germany

[24] Dipartimento di Chimica, Biologia e Biotecnologie, Università degli Studi e INFN, 06123 Perugia, Italy

[25] Amherst Center for Fundamental Interactions and Physics Department, University of Massachusetts, Amherst, MA 01003, USA

[26] Physics and Astronomy Department, University of California Los Angeles (UCLA), Los Angeles, California 90095, USA

Abstract. Borexino is a 300 ton sub-MeV liquid scintillator solar neutrino detector which has been running at the Laboratori Nazionali del Gran Sasso (Italy) since 2007. Thanks to its unprecedented radio-purity, it was able to measure the flux of ^{7}Be, ^{8}B, pp, and pep solar neutrinos and to detect geo-neutrinos. A reliable simulation of the detector is an invaluable tool for all Borexino physics analyses. The simulation accounts for the energy loss of particles in all the detector components, the generation of the scintillation photons, their propagation within the liquid scintillator volume, and a detailed simulation of the electronics chain. A novel efficient method for simulating the external background which survives the Borexino passive shield was developed. This technique allows to reliably predict the effect of the contamination in the peripheral construction materials. The techniques developed to simulate the Borexino detector and their level of refinement are of possible interest to the neutrino and dark matter communities, especially for current and future large-volume liquid scintillator experiments.

1. Introduction

Borexino pioneered the development of ultra-low radioactive background detectors twenty-five years ago. The usage of a large volume, liquid scintillator detector made the measurement of most of the solar neutrino spectrum possible [1, 2]. Besides Borexino, a large number of liquid scintillator detectors were operated, are running, or are being designed for measurements on neutrino oscillations, neutrinoless double beta decay, or for use as active γ-ray and neutron veto devices for direct WIMP dark matter experiments (see Tab. 1 of Ref. [3]). The accurate modeling of the detector response by means of Monte Carlo (MC) methods is pivotal to perform precise and high quality measurements. In this paper, the MC simulation of the Borexino experiment is described. The methods and the results here illustrated can be easily adapted to other liquid scintillators and detector geometries. This work is fundamentally based on Ref. [3].

2. The Borexino experiment

Borexino is an un-segmented calorimeter consisting of $\sim$278 t of organic liquid scintillator [4]. It is schematically depicted in the left panel of Fig. 1. The inner detector is enclosed by a stainless steel sphere (SSS) that serves both as the container of the scintillator and as the mechanical support of the photomultipliers (PMTs). Within this sphere, two nylon vessels (0.125 mm thick) separate the volume in three shells of radii 4.25 m, 5.50 m, and 6.85 m. The inner nylon vessel contains the liquid scintillator solution, namely PC (pseudocumene) as a solvent and the fluor
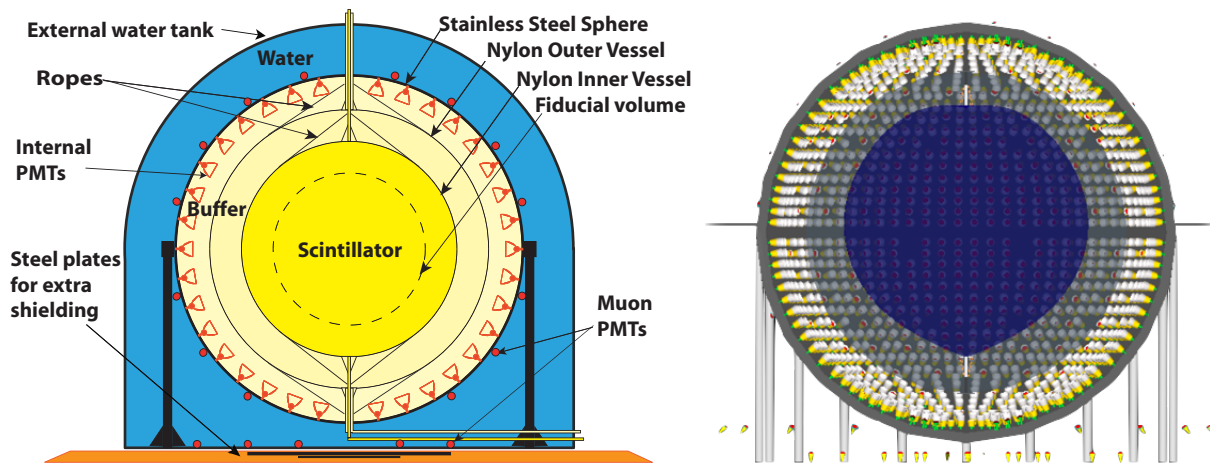
Figure 1. *Left Panel:* Schematic drawing of the Borexino detector. *Right Panel:* Cross section of the detector geometry as implemented in the simulation.

PPO (2,5-diphenyloxazole) as a solute at a concentration of 1.5 g/l. The second and the third shells (buffer regions) contain PC with a small amount (2.8 g/l) of DMP (dimethylphthalate) as a light quencher added to further reduce the scintillation yield of pure PC. 2212 internal PMTs mounted on the inner side of the stainless steel sphere detect the scintillation light. A 18 m in diameter, 16.9 m height domed cylinder filled by ultra-pure water contains the SSS and acts both as radiation shielding and as Čerenkov detector for identifying and vetoing cosmic muons. For this purpose, 208 additional PMTs are mounted on the outer side of the SSS and on the water tank floor. Solar neutrinos are detected through their elastic scattering on electrons. The measurement of different solar neutrino components is possible through a fit of the electron recoil energy spectrum, which can disentangle the contribution of solar neutrinos and that of background signals [2]. Anti-neutrinos ($\bar{\nu}_e$) are detected via inverse β decay ($\bar{\nu}_e + p \rightarrow e^+ + n$) with a threshold of 1.806 MeV. The characteristic time and spatial coincidences of prompt (positron energy depositions) and delayed events (neutron capture) offer a clean signature for the $\bar{\nu}_e$ detection.

Borexino was designed (and then succeeded) to measure the low energy portion of the solar neutrino spectrum and, in particular, the 0.862 MeV ^{7}Be solar neutrinos [5, 6]. The extremely low levels of radioactivity achieved within the scintillator allowed Borexino to broaden its science reach beyond the original design goal. Borexino reported the first evidence for pep neutrinos and the best upper limit on the solar CNO flux [7], as well as the measurement of the electron recoil induced by ^{8}B neutrinos with a record-low threshold of 3 MeV [8], and the first real-time detection of pp solar neutrinos [9]. Further physics results of Borexino include the detection of geo-neutrinos [10], searches for anti-neutrinos from astrophysical sources up to 15 MeV [11, 12], searches for solar axions at 5.5 MeV [13], as well as other exotic searches [14, 15, 16]. The investigation of short baseline anti-neutrino oscillations into light sterile neutrinos using an artificial ^{144}Ce-^{144}Pr source is planned for the near future within the SOX project [17].

The precision level of the Borexino MC simulation described in Ref. [3] and here summarized, was fundamental for the development of the improved analyses on ^{7}Be, pep, pp, CNO, and ^{8}B solar neutrinos which were recently reported in Refs. [18, 19].

3. The Monte Carlo simulation code

The Borexino MC simulation was designed and optimized to fully model and reproduce particle energy deposition, scintillation and Čerenkov photon production, and light propagation in all the detector volume up to the signal detection [3, 20]. The event and light generation as well as light propagation are implemented within the Geant4 package and use the standard libraries therein [21]. Once optical photons reach the PMTs, a detailed electronics simulation takes place, accurately modeling detector response and trigger formation.

The first ingredient for a successful MC is a detailed geometry and material simulation. The right panel of Fig. 1 shows a cross section of Borexino as implemented in the simulation. All the most relevant geometrical features are included, such as the PMTs with their real shapes and positions, the nylon vessels, and the holding endcaps. The water tank geometry is also accurately reproduced. Besides the geometrical details implemented in the simulation, the optical properties of all the materials involved are considered according to specific measurements or data available in the literature. It has to be noted that the inner nylon vessel shape is time dependent [2] and this is properly accounted for in the simulation [3].

3.1. Event generation

Several generators were developed to simulate radioactive decays inside the scintillator, solar neutrinos, and radioactive sources encapsulated as in the calibration campaign [22]. Standard Geant4 classes manage most of the radioactive decays. Solar neutrino interactions are generated with a custom algorithm based on the spectra as computed in the Standard Solar Model and the standard electroweak theory considering neutrino oscillations. The propagation of γ-rays from the SSS to the innermost fiducial volume is performed exploiting a novel technique, briefly presented in Sec. 3.4 and more widely discussed in Refs. [3, 20].

3.2. Optical photon generation and propagation

The number of emitted photons and their time distribution in the PC+PPO mixture depend on the details of the charged particle energy loss processes and on the molecular interactions between solvent and fluor in the scintillator. The light quenching due to ionization is modeled by the Birks formula [23] that links the scintillation light yield to the particle stopping power. A correct parametrization of the Birks formalism requires to make the model compatible with the Geant4 framework, by evaluating the quenching factor for the primary ionizing particle, and making each daughter inherit the same factor [3]. The primary spectrum of Čerenkov light is simulated by generating a number of photons per unit length and wavelength according to the Frank-Tamm equation [24]. An accurate knowledge of the scintillator index of refraction is needed for a successful Čerenkov light simulation.

The Borexino MC tracks each optical photon individually, considering its interactions with the single components of the scintillator and the buffer. These processes include elastic Rayleigh scattering, absorption and reemission by PPO, absorption by DMP, and also photon absorption in the thin nylon vessels. The wavelength dependent attenuation lengths for these interactions were obtained with dedicated spectrophotometric measurements. The absorption and reemission models adopted in Borexino's simulation treat separately the different components of the scintillator mix (PC, PPO, and DMP) [3].

3.3. Electronics simulation

The electronics simulation code reproduces the electronics chain and the trigger system response, based on the information of the PMT pulse times recorded in the Geant4 simulation. The code simulates the detector electronics following its operating status over the entire data taking period [3]. The dark rate of individual PMTs, the effective quantum efficiency for each channel, and the PMT gains are saved in a database and are injected in the simulation on a weekly
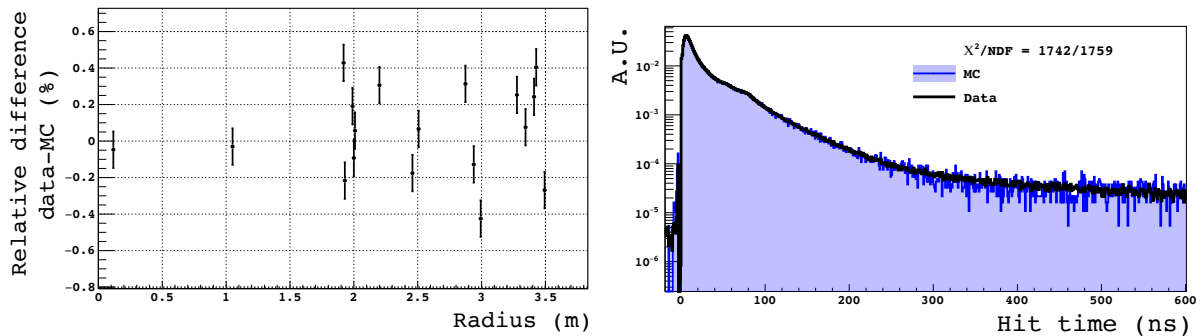
Figure 2.   *Left Panel:* Relative difference of the energy peak position in MC and data (N_h energy estimator) for calibration events as a function of the radial distance of the source from the center [3]. *Right Panel:* Light curve (i. e. hit times with respect to the first hit in the cluster) for calibration events in the center of the detector [3].

basis. In addition, the code includes the effect of bad channels and detector inefficiencies by default in the same time dependent way. The charge associated to each photoelectron is sampled from the single photoelectron response of each PMT modeled as an exponential plus Gaussian distribution. The specific parameters describing this curve for each PMT were measured channel by channel [3]. MC event reconstruction is performed in the same way as data [2].

3.4. External background simulation

An appropriate understanding of the external background was achieved by combining the information obtained from the external calibration of the detector [22] with the development of a special simulation procedure for the γ-rays originating in the PMTs and in the SSS. The rate of the external γ-rays reaching a fiducial sphere of 3 m radius is reduced by a factor $\sim 10^7$ thanks to the scintillator self-shielding. This makes it computationally unpractical to simply simulate the γ-rays transport in the standard framework. Therefore, we implemented an importance sampling algorithm [21] as variance reduction technique to speed up the simulation. The algorithm considers the volume surrounded by the SSS as divided into spherical concentric shells. Every time a photon crosses a boundary between two shells, the particle is either split or killed with a given probability depending on whether the "importance" of the entering volume is higher or lower than the exiting one. The importance grows while going towards the center of the detector: this makes it more favorable for gammas to reach the innermost fiducial volume. This algorithm simulates external background events originated on the SSS and interacting inside the 3 m spherical fiducial volume at a rate of about 0.5 events per second. More details can be found in Refs. [20, 3].

4. Tuning and validation

The MC was tuned and validated using data sets independent from the ones used for physics analyses. The most important features of the events, i. e. the time-related distributions and the position-dependent number of hits and photoelectrons detected by each PMT, are reproduced with an accuracy of better than 1% within a 3 m radius fiducial volume in the energy range of solar neutrino analyses [3]. The full simulations of scintillation and light propagation require the input of a large number of parameters describing various features of the scintillator and of the materials. The calibration campaigns [22] provided clean data samples to optimize the simulation. A portion of the calibration data was used as a tuning sample, while an independent set of calibration data was used for testing the performance of the simulation. The main difficulty
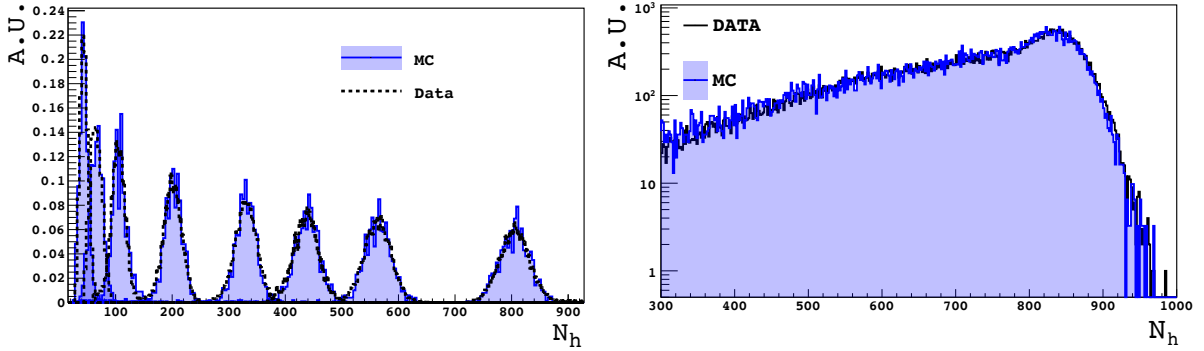
Figure 3. *Left panel:* Data-MC agreement for the N_h energy estimator for different gamma source energies in the center of the detector. *Right panel:* Comparison of the external γ-ray energy spectrum (N_h) for source-induced events from the external calibration campaign. The fiducial volume is defined as a sphere with 3.5 m radius.

in the tuning procedure is posed by the correlations among the parameters. Most of the physical effects (which are connected to the material properties) are mutually dependent. More details on the parameter tuning procedure can be found in Refs. [20, 3].

One of the critical aspects of the simulation is the reproduction of the detector response non-uniformities for events in different positions in the fiducial volume. For solar neutrino analyses, the goal is $\lesssim 1\%$ and the comparison between data and simulation is shown in the left panel of Fig. 2, where the relative discrepancy for the energy estimator N_h (the number of hits collected by the PMTs, see Ref. [2]) for calibration events is plotted as a function of the source radial position. Inside a 3.5 m sphere, all the points are contained in the $\pm 0.5\%$ band, thus showing that the precision goal was reached. The right panel of Fig. 2 compares the MC and data time distribution of the hits detected by the PMTs for calibration source events in the center. This curve is the convolution of the four exponential response function used to describe the scintillation process (see Ref. [2]) and the simulated absorptions and reemissions. The correct reproduction of the hit time distribution ensures that other more complex variables reconstructed from the hit times are also correctly reproduced by the MC. The reproduction of the energy response for β particles was optimized scanning the light yield, the Birks quenching factor, the optical photon reemission probability at low wavelengths, and an overall multiplicative parameter rescaling the simulated single photoelectron gains of the PMTs [3]. A comparison of the calibration γ-ray source peak positions for the N_h variable is shown in the left panel of Fig. 3. The energy response (peak and resolution) of all the sources located in the center of the detector is reproduced with a precision better than 0.8% [3]. The external γ-ray simulation procedure described in Sec. 3.4 was validated by direct comparison with data from calibrations [3, 22]. The reconstructed energy spectra and event positions were compared to the measured ones, recording an excellent agreement. In particular, the right panel of Fig. 3 shows the agreement in the energy spectrum for external γ-ray events in a 3.5 m fiducial volume sphere.

5. Event pileup simulation

Pileup events are due to two or more scintillation events happening so close in time that the clustering algorithm cannot disentangle them. It is the most critical background for very low energy solar neutrino analyses, particularly for the measurement of the pp neutrino interaction rate [9]. It is possible to build the pileup energy spectrum using a data driven method ("synthetic pileup") [9]. The synthetic pileup production considers the hits recorded within a specific time interval in the second half of the acquisition gate and superimposes them with the primary

cluster, which caused the trigger to occur and is placed at the beginning of the DAQ gate. These synthetic events are then processed with the standard reconstruction code. The tuned MC simulation allows to reproduce the synthetic pileup and to gain understanding on its different components. Details on the implementation can be found in Refs. [20, 3].

6. Conclusions and outlook

The most recent developments of the Borexino Monte Carlo ab initio simulation allowed to reach an accuracy better than 1% in all the relevant quantities for solar physics analyses. The usage of calibration sources proved to be essential in providing a large statistical sample of events with well-defined energies and positions. These data sets allowed a precise tuning and validation of the simulation as a whole. Novel simulation approaches for an efficient and accurate simulation of external backgrounds were developed. These enabled to further understand crucial backgrounds in Borexino such as external γ-rays and event pileup.

The Borexino MC code is an invaluable tool for all physics analyses and the results presented in Refs. [18, 19] demonstrate it. Future possible developments include improvements in the data-MC agreement at higher energies and larger radii, aiming at even better performances to be exploited within the SOX experiment.

References

[1] R. S. Raghavan, S. Pakvasa and B. A. Brown, Phys. Rev. Lett. **57**, 1801 (1986). doi:10.1103/PhysRevLett.57.1801

[2] G. Bellini *et al.* [Borexino Collaboration], Phys. Rev. D **89**, no. 11, 112007 (2014) doi:10.1103/PhysRevD.89.112007.

[3] M. Agostini *et al.* [Borexino Collaboration], *Preprint:* arXiv:1704.02291 [physics.ins-det], *Accepted for publication on "Astroparticle Physics"*.

[4] G. Alimonti *et al.* [Borexino Collaboration], Nucl. Instrum. Meth. A **600**, 568 (2009) doi:10.1016/j.nima.2008.11.076 (*Preprint:* arXiv:0806.2400 [physics.ins-det]).

[5] G. Bellini *et al.*, Phys. Rev. Lett. **107**, 141302 (2011) doi:10.1103/PhysRevLett.107.141302 (*Preprint:* arXiv:1104.1816 [hep-ex]).

[6] G. Bellini *et al.* [Borexino Collaboration], Phys. Lett. B **707**, 22 (2012) doi:10.1016/j.physletb.2011.11.025 (*Preprint:* arXiv:1104.2150 [hep-ex]).

[7] G. Bellini *et al.* [Borexino Collaboration], Phys. Rev. Lett. **108**, 051302 (2012) doi:10.1103/PhysRevLett.108.051302 (*Preprint:* arXiv:1110.3230 [hep-ex]).

[8] G. Bellini *et al.* [Borexino Collaboration], Phys. Rev. D **82**, 033006 (2010) doi:10.1103/PhysRevD.82.033006 (*Preprint:* arXiv:0808.2868 [astro-ph]).

[9] G. Bellini *et al.* [Borexino Collaboration], Nature **512**, no. 7515, 383 (2014). doi:10.1038/nature13702

[10] M. Agostini *et al.* [Borexino Collaboration], Phys. Rev. D **92**, no. 3, 031101 (2015) doi:10.1103/PhysRevD.92.031101 (*Preprint:* arXiv:1506.04610 [hep-ex]).

[11] G. Bellini *et al.* [Borexino Collaboration], Phys. Lett. B **696**, 191 (2011) doi:10.1016/j.physletb.2010.12.030 (*Preprint:* arXiv:1010.0029 [hep-ex]).

[12] M. Agostini *et al.* [Borexino Collaboration], Astropart. Phys. **86**, 11 (2017) doi:10.1016/j.astropartphys.2016.10.004 (*Preprint:* arXiv:1607.05649 [astro-ph.HE]).

[13] G. Bellini *et al.* [Borexino Collaboration], Phys. Rev. D **85**, 092003 (2012) doi:10.1103/PhysRevD.85.092003 (*Preprint:* arXiv:1203.6258 [hep-ex]).

[14] M. Agostini *et al.* [Borexino Collaboration], Phys. Rev. Lett. **115**, 231802 (2015) doi:10.1103/PhysRevLett.115.231802 (*Preprint:* arXiv:1509.01223 [hep-ex]).

[15] G. Bellini *et al.* [Borexino Collaboration], Phys. Rev. C **81**, 034317 (2010) doi:10.1103/PhysRevC.81.034317 (*Preprint:* arXiv:0911.0548 [hep-ex]).

[16] G. Bellini *et al.* [Borexino Collaboration], Phys. Rev. D **88**, no. 7, 072010 (2013) doi:10.1103/PhysRevD.88.072010 (*Preprint:* arXiv:1311.5347 [hep-ex]).

[17] G. Bellini *et al.* [Borexino Collaboration], JHEP **1308**, 038 (2013) doi:10.1007/JHEP08(2013)038 (*Preprint:* arXiv:1304.7721 [physics.ins-det]).

[18] M. Agostini *et al.* [Borexino Collaboration], *Preprint:* arXiv:1707.09279 [hep-ex].

[19] M. Agostini *et al.* [Borexino Collaboration], *Preprint:* arXiv:1709.00756 [hep-ex].

[20] S. Marcocci, *"Precision Measurement of Solar ν Fluxes with Borexino and Prospects for $0\nu\beta\beta$ Search with ^{136}Xe-loaded Liquid Scintillators"*, PhD thesis, Gran Sasso Science Institute, 2016.

[21] S. Agostinelli *et al.* [GEANT4 Collaboration], Nucl. Instrum. Meth. A **506**, 250 (2003). doi:10.1016/S0168-9002(03)01368-8

[22] H. Back *et al.* [Borexino Collaboration], JINST **7**, P10018 (2012) doi:10.1088/1748-0221/7/10/P10018 (*Preprint:* arXiv:1207.4816 [physics.ins-det]).

[23] J. B. Birks, Proc. Phys. Soc. A **64**, 874 (1951). doi:10.1088/0370-1298/64/10/303

[24] K. A. Olive *et al.* [Particle Data Group], Chin. Phys. C **38**, 090001 (2014). doi:10.1088/1674-1137/38/9/090001